Chapter 5

Iron Based Shape Memory Alloys: Mechanical and Structural Properties

Fabiana Cristina Nascimento Borges

Additional information is available at the end of the chapter

http://dx.doi.org/10.5772/51877

1. Introduction

The technological development is one of the reasons why there is a variety of new materials that can be applied to various situations. This situation enables many materials to be applied in different areas: engineering, medicine, agriculture, arts, space field, among others. Alloys with shape memory effect (SME) are materials that exhibit interesting characteristics and can be applied in various situations.

The SME in Fe-based alloys results from the reverse motion of Shockley partial dislocation during heating (Otubo, 2002) and (Bergeon et al. 1997). Figure 1 shows a schematic figure of

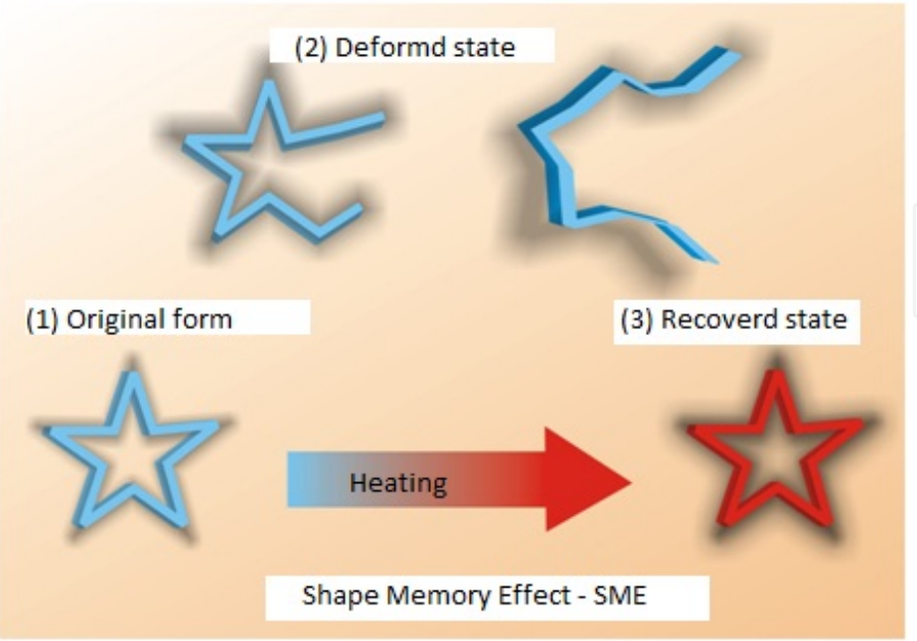

Figure 1. Shape Memory Effect (Nascimento, 2008).

SME. The original form of the material is a star, Fig. 1-(1). This star is deformed beyond its elastic limit, Fig. 1-(2) and the original crystal structure (f.c.c.) is transformed into h.c.p. structure. During the heating, reversion to the f.c.c. structure occurs and the original shape is recovered Fig. 1-(3). Reversion to the matrix phase (austenite) is not complete because a martensite residual amount exists which is not recovered during the heat treatment. Chemical composition and austenite grain size are important factors that affect the shape recovery in iron based shape memory alloys.

In this study, structural parameters of stress induced ε-martensite were analyzed for Fe-Mn-Si-Cr-Ni-(Co) different chemical compositions. The material was hot rolled at 1473 K followed by a heat-treatment at 1323 K for different times to obtain different austenite grain sizes samples. Two parameters were considered: austenitic grain and training cycles.

2. Iron shape memory alloys – history

Iron based shape memory alloys have been largely investigated during the last years. The Shape Memory Effect (SME) is a physical phenomenon which results in recovery of the original shape through temperature variation after the material has been deformed beyond its elastic limit. The alloys that exhibit this characteristic are known as Smart Materials - a group of materials that show reproducible and stable responses, through significant variations of at least one property, when subjected to external stimuli. Table 1 shows some of these materials and their properties.

In iron based alloys the SME, is related with the γ(f.c.c.) ↔ ε(h.c.p.) nonthermoelastic martensitic transformation (Bergeon et al. 1997). This effect is the result of the reverse motion of Shockley partial dislocation during heating. In general, the technological development was largely responsible for, the emergence of new compositions with SME. The ferrous alloy was developed as an alternative to NiTi alloys and also the copper base compositions due to its low cost and properties similar to nitinol alloy.

Fe-Mn-Si alloys began to be studied in the 80s (Sato et al. 1982). The alloying elements Cr, Ni and Co were subsequently used to improve the properties of shape recovery. Fe-Mn-Si-Cr-Ni-Co alloys were developed, with several attractive properties and a more desirable shape recovery making them suitable for various technological applications (Shiming et al. 1991), (Bergeon et al. 1997), (Kajiwara et al. 1999), (Arruda, 1999). In Brazil the family of iron-based shape memory alloys has been extensively studied since 1995 (Otubo et al. 1995).

Tab. 2 presents a list of research groups registered in the CNPq (National Counsel of Technological and Scientific Development) investigating the ferrous alloys with EMF in Brazil.

Research groups are listed in Tab. 2 to present the several technological applications and basic studies. In this study we will focus on recovery as a function of the initial microstructure and training cycles.

Smart Materials	Properties
Shape memory alloys and shape memory polymers	Materials in which large deformation can be induced and recovered through temperature changes or stress changes.
Magnetic shape memory alloys	Materials that change their shape in response to significant change in the magnetic field.
Piezoelectric materials	Materials that produce a voltage when stress is applied.
Magnetostrictive materials	Materials that exhibit change in shape under the influence of magnetic field.
pH-sensitive polymers	Materials that change in volume when the pH of the surrounding medium changes.
Temperature-responsive polymers	Materials which undergo changes upon temperature.
Halochromic materials	Materials that change their color as a result of changing acidity.
Chromogenic systems	Materials that change color in response to electrical, optical or thermal changes.
Ferrofluid	
Photomechanical materials	Materials that change shape under exposure to light.
Self-healing materials	Materials that have the intrinsic ability to repair damage due to normal usage, thus expanding the material's lifetime
Dielectric elastomers	Smart material systems which produce large strains (up to 300%) under the influence of an external electric field.
Magnetocaloric materials	Compounds that undergo a reversible change in temperature upon exposure to a changing magnetic field.
Thermoelectric materials	Materials used to build devices that convert temperature differences into electricity and vice-versa.

Table 1. Smart Materials

Research groups -source: CNPq	Identification	Iron-based alloy
Development of metallic alloys	Fundação Centro Tecnológico de Minas Gerais – *CETEC*	Fe-Mn-Si-(Ni-Cr-Co)
Development of metallic alloys for industrial applications	Universidade Estadual de Campinas – *UNICAMP*	Fe-Mn-Si-(Ni-Cr-Co)
Shape memory alloys - characterization and application	Universidade Estadual de Ponta Grossa – *UEPG*	Fe-Mn-Si-Ni-Cr-(Co) and NiTi
Shape memory materials	Instituto Tecnológico da Aeronáutica – *ITA*	Stainless steel e NiTi

Table 2. Research groups of iron shape memory alloy in Brazil (source: CNPq)

3. Structural and mechanical properties

Technological applications of these alloys are directly related to the study of their mechanical and structural properties. There are several mechanical properties which may be mentioned. In this study the relationship between the effect of structural parameters on the mechanical properties and shape recovery will be presented through the analysis of samples subjected to cycles of training using compression test. Therefore, the results discussed refer to the reverse transformation of stress induced ε-martensite.

3.1. Structural characterizations

As it is known, the SME is directly related to processing and reversing the crystalline phases. In these materials the following transformations may occur:

$$g\left(f.c.c.\right) \leftrightarrow \left(h.c.p.\right), \gamma\left(f.c.c.\right) \leftrightarrow \alpha'\left(b.c.c.\right) \text{ and } \gamma\left(f.c.c.\right)\varepsilon\left(h.c.p.\right) \leftrightarrow \alpha'\left(b.c.c.\right)$$

The predominant type of transformation will depend on factors such as chemical composition and thermomechanical treatment cycles. The α' phase is bcc; Shockley partial dislocations are specific of compact structures f.c.c. and h.c.p. When the fraction of b.c.c. phase increases, there is a decrease in the fraction of compact structures, thus the recovery mechanism through partial dislocation Shockley is smaller.

The three types of crystal structure show interesting peculiarities which are discussed below.

a. Austenitic phase

The austenitic phase in iron based Fe alloys is known as a strong and stable phase. Crystallographically it presents characteristics similar to commercial stainless steels, AISI 304. It features a cubic crystal structure (f.c.c.) and space group Fm-3m.

b. Martensitic phase

In this study there are two important phases resulting from the martensitic transformation:

$$\gamma\left(f.c.c.\right)\rightarrow\varepsilon\left(h.c.p.\right)\rightarrow\alpha'\left(b.c.c.\right)or\,\gamma\left(f.c.c.\right)\rightarrow\alpha'\left(b.c.c.\right)$$

The ε-martensite-phase is of greater interest because the reversion to austenite results in SME. Literature data show that the hexagonal structure (h.c.p.) can be mechanically or thermally induced. In particular in this case priority is given for the stress induced ε-martensite.

The atomic stacking sequence for the f.c.c. phase is ABCABCABC ... and h.c.p. phase is ABABAB. According to studies on stacking faults, they are necessary in the f.c.c structure in order to generate the embryos which form the martensitic phase. The overlapping of stacking faults form an h.c.p. volume and a reversal movement of Shockley partial dislocation occurs. Figure 2 shows a diagram of the stacking sequence to cubic and hexagonal structures. The orientation relationship between these phases is shown in Figure 3.

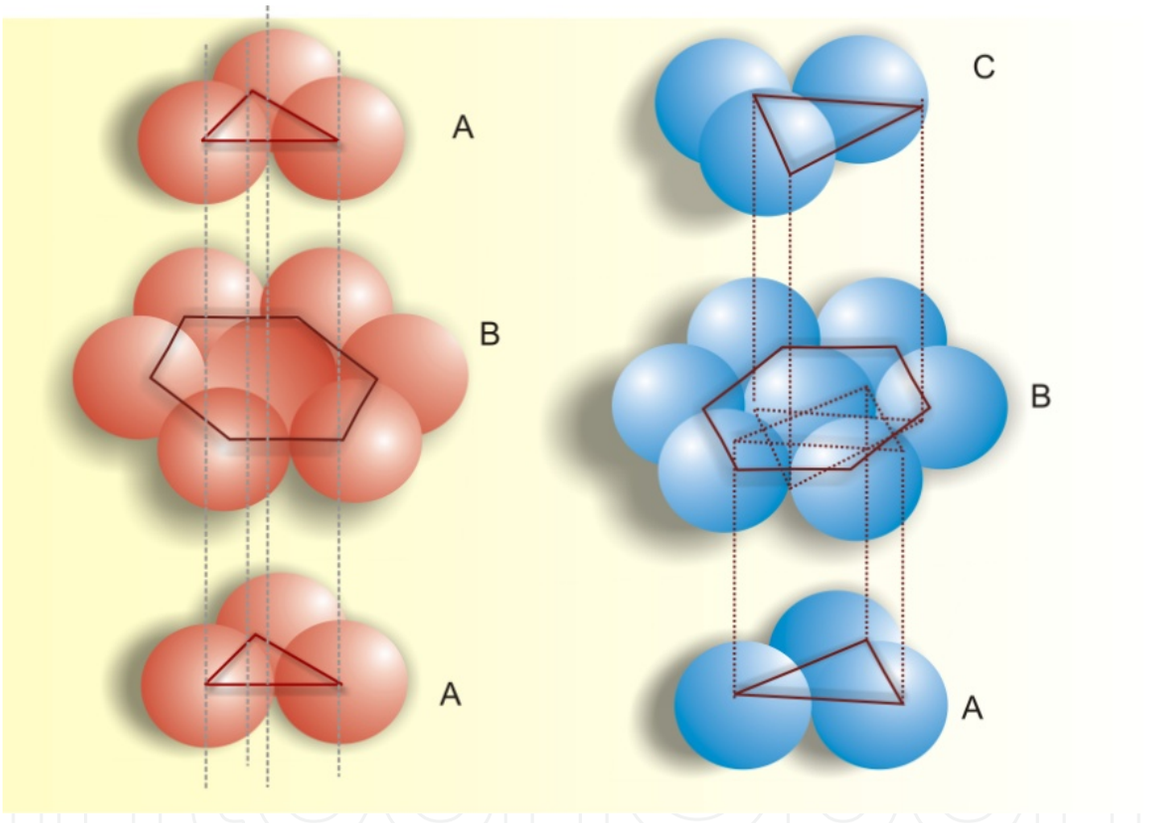

Figure 2. Atomic stacking sequence (ABCABCABC...) for f.c.c. structure with overlapping every third crystal plane (111) along [111]. Atomic stacking sequence (ABABAB...) for h.c.p. structure with overlapping crystal planes (0001) alternate along [0001] (Van Vlack, 1998).

The martensite and austenite phases can be identified using different techniques such as X-ray diffraction (XRD) and optical microscopy. The ferrous alloys, with SME, present a diffractogram similiar to AISI 304 commercial austenitic steels. Table 3 shows the position of 2θ reflections corresponding to the martensite and austenite phases. In this study, the XRD data were collected between 10 and 100°(2θ) at room temperature using a Philips diffractometer (PW1710) with Cu target and a graphite diffracted beam monochromator, step sizes of 0.02° and 2 seconds counting time.

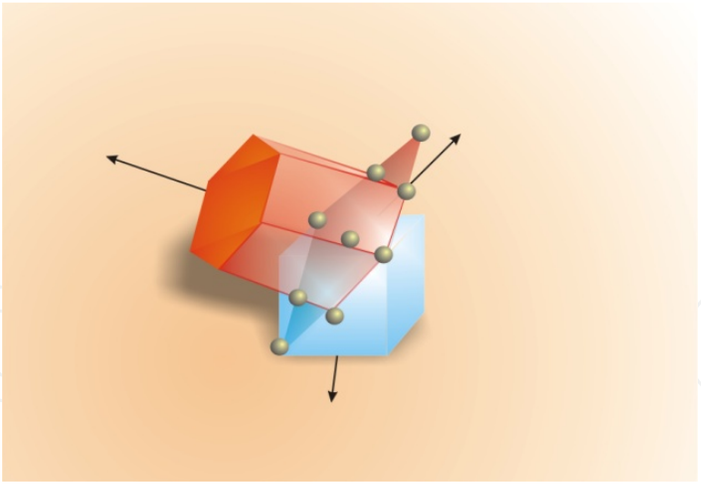

Figure 3. Orientation relationship between h.c.p. and f.c.c. phases (Huijun 1999).

Phase	(h.k.l.)	2θ
γ-austenite	(111)	43.7
Structure: cubic	(200)	50.7
Space group: Fm-3m	(220)	74.8
	(311)	90.8
ε-martensite	(10.0)	41.0
Structure: hexagonal	(10.1)	46.9
Space group: $P6_3/mm6$ ($\gamma = 120^o$)	(10.2)	62.0

Table 3. Identification of austenite and martensite phases.

Figure 4 shows the identification of these phases and the effect of the training cycle on a sample with grain size 75 μm (4 - ASTM).

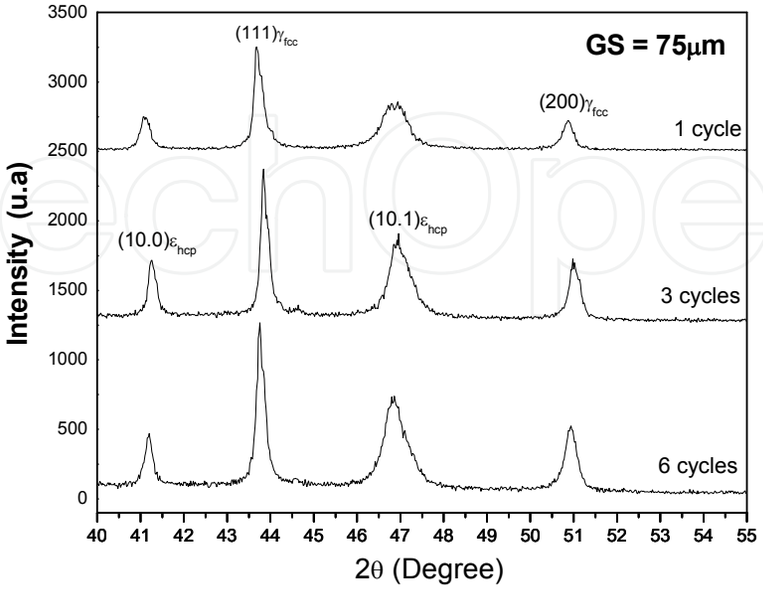

Figure 4. XRD patterns for 1st, 3rd and 6th thermo-mechanical cycles, deformed state, GS = 75 μm (Nascimento et al. 2008).

Figure 4 shows that with the increasing number of training cycles, the volumetric fraction of the martensitic phase increases. Using Rietveld refinement the quantitative analysis of phases was estimated considering the integrated intensity of the peaks $(10.1)_{\varepsilon}$ The small shift in the position 2θ of reflection (111)-austenitic phase shows variations in the lattice parameter of the unit cell this phase. These changes can be analyzed using Rietveld refinement.

In the Rietveld refinement the peak shape, width parameters and background parameters are considered. All these parameters were refined adopting the iterative least-squares method through minimization of residual parameter. Two structure types were considered: (a) cubic symmetry, space group **Fm-3m** for austenite phase, and (b) hexagonal symmetry, space group **P63/mmc** (with γ = 120°) for the martensite phase. Lattice parameters correspond to a similar composition alloy, AISI-304 steel. The thermal parameters (B's) initially used for both phases were $B_{overall}$ = 0.5 and the peak shape function used was the pseudo-Voigt. Figure 5 presents the experimental and refined X ray diffraction patterns as well as their difference.

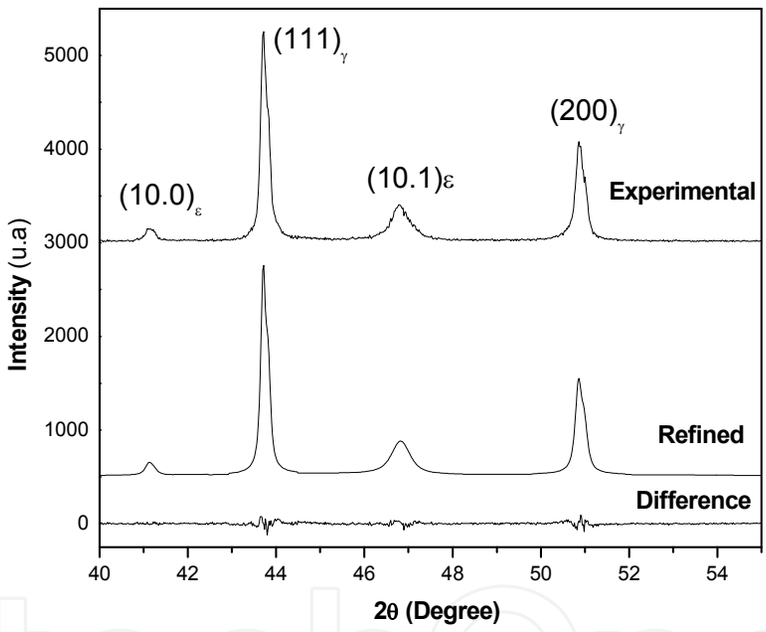

Figure 5. Rietveld refinement (GS = 75 μm), last thermo-mechanical cycle, deformed state (Nascimento et al. 2008).

The ε-martensite lattice parameters for the first cycle were: a_{ε} = 2.548(6) Å, c_{ε} = 4.162(2) Å. The ratio c/a found was c/a = 1.633(2). The standard deviations are shown in parenthesis. Austenitic phase indicated lattice parameters similar to those presented in the literature for stainless steel (Gauzzi et al. 1999): a_{γ} = 3.587(2) Å. Lattice parameters for the austenitic phase presented small variations (< 3%). The discrepancies between the experimental and refined profiles for all samples are small, indicating that the unit cell dimensions were accurately determined and that the chosen peak shape function pseudo-Voigt was a good choice for these samples. The thermal parameters (B's) presented a variation smaller than 0.5%. These structural variations are important because they affect the ratio c/a and also the reversion to the cubic austenitic phase (Nascimento et al. 2008).

Previous studies (Nascimento et al. 2008) show the effect of training cycles on the lattice parameter of the unit cell in stainless shape memory alloy, Figure 6. We note that for the sample with smaller grain size (75 μm) the a-parameters decreased with increased training cycles while the c-parameter increased. These changes affect the SME.

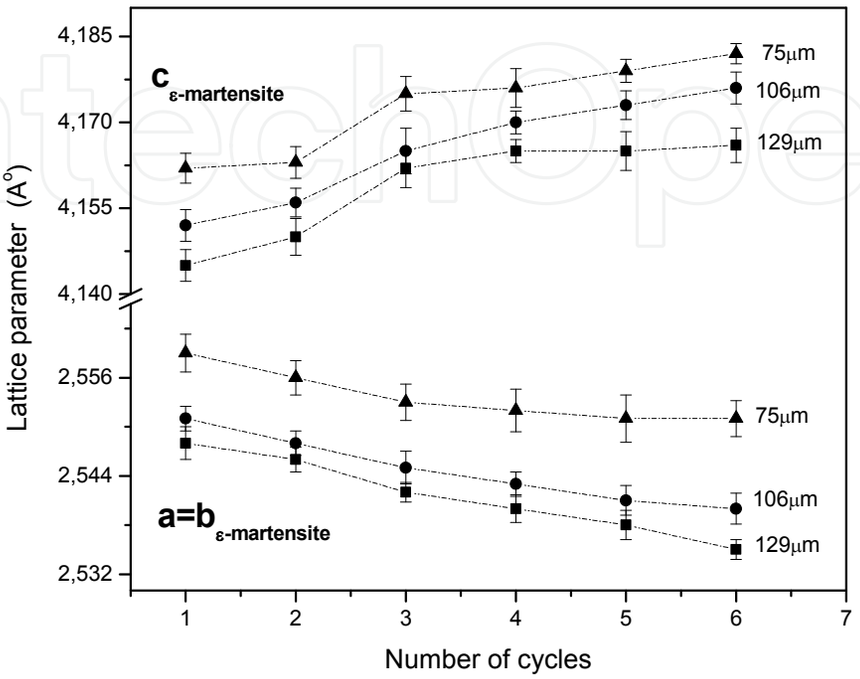

Figure 6. Structural parameters variation for austenite and martensite phases as a function of training cycles and grain size (Nascimento et al. 2008).

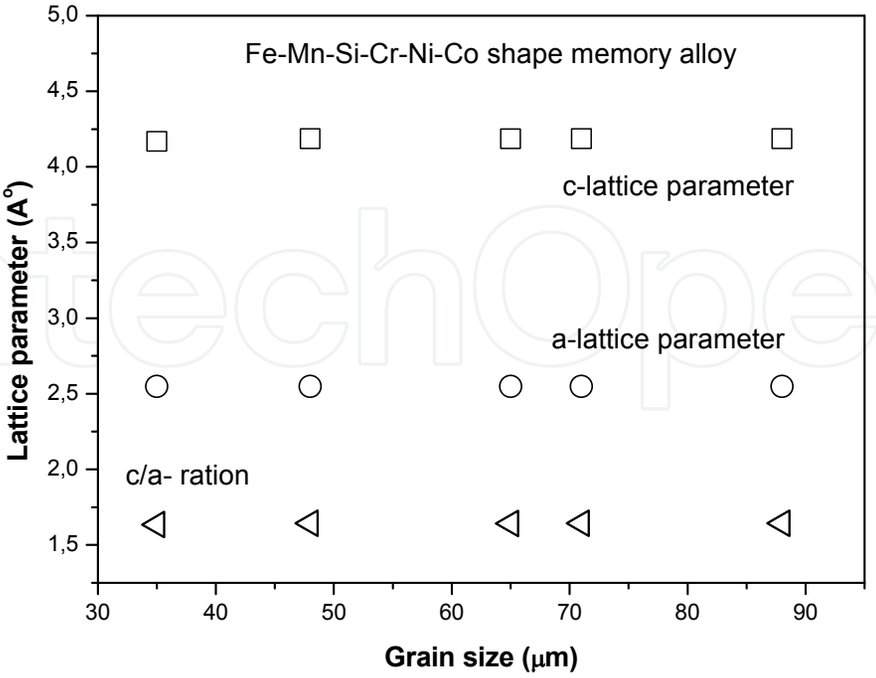

Figure 7. Structural parameters variation for austenite and martensite phases as a function of the grain size.

Figure 7 shows the variation of the structural parameters a, c, and the ratio a/c as a function of the initial microstructure. These samples showed a smaller variation of grain size and consequently lower variation of structural parameters.

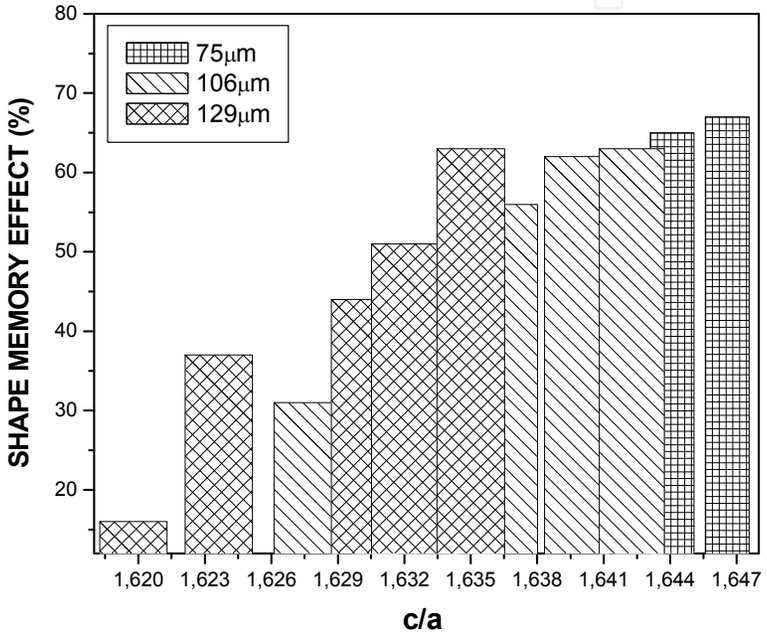

Figure 8. Shape memory effect as a function of ratio c/a.

Another way to identify the phases in alloys with SME is through optical microscopy using specific etching. The phases are differentiated through color (color etching method) that should be adapted to each sample (Nascimento et al. 2003). Figure 9 shows some images of the Fe-Mn-Si-Cr-Ni-Co alloy. In the first image, the austenitic grain boundaries are seen (Fig. 9a). Austenitic grain orientations are observed by different colors. Deformation twins can also be viewed (Fig. 9b). The coexistence of martensite and austenite phases can be observed in Fig. 9c. In this case, the darker regions have been identified as the martensitic phase. The color etching is also very important to verify the presence of the α'-martensite, considered as detrimental to the shape recovery process. This phase was not identified by X-ray diffraction because it has a low volumetric fraction (<2%). But, using optical microscopy, the α'-martensite was identified as spots throughout the sheets of ε-martensite, Fig. 9d.

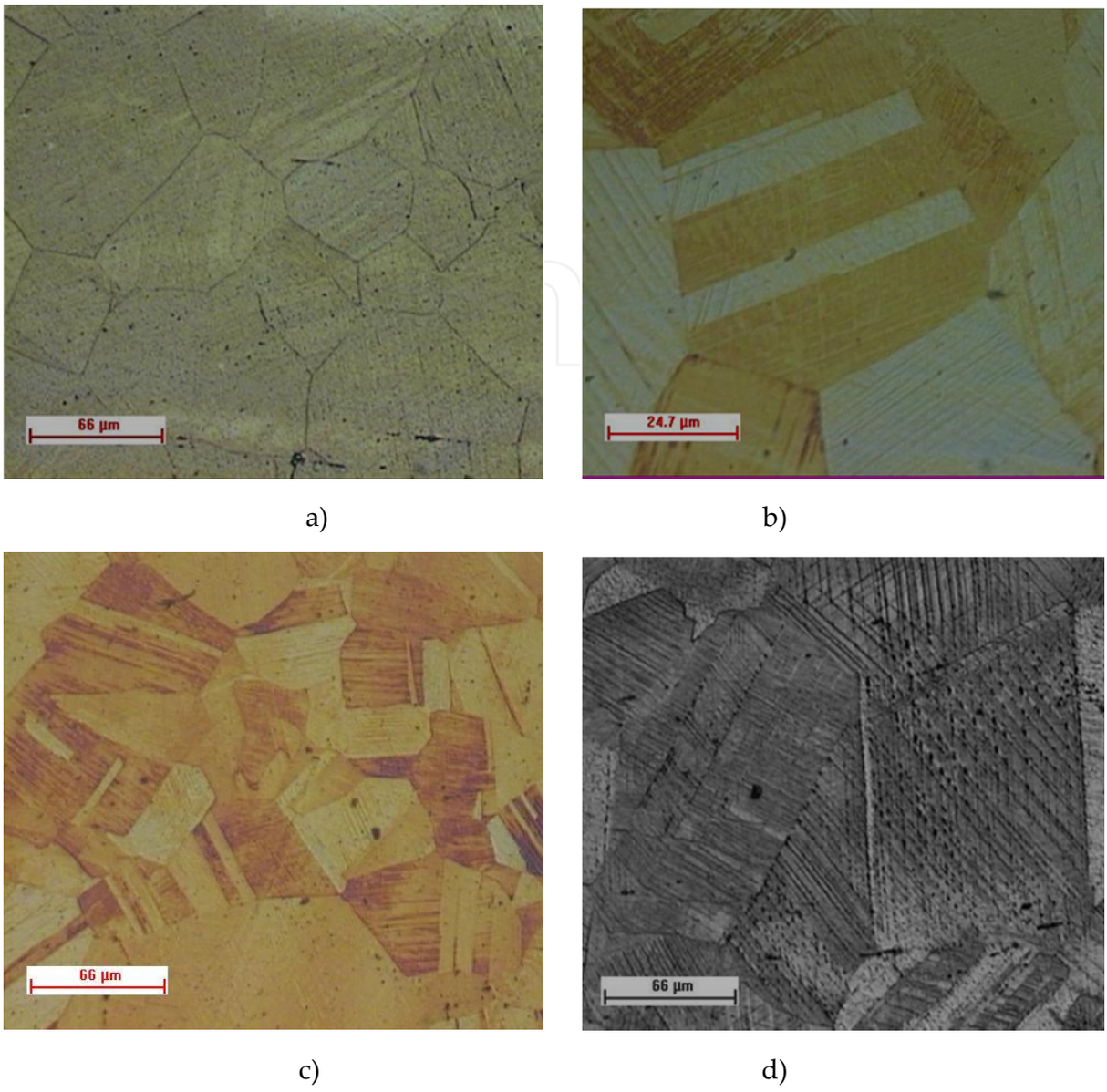

Figure 9. Identification of martensite and austenite phases using color etching: 2.0 g $K_2S_2O_5$ + 0.5g NH_4HF_2 + 50 ml H_2O (Bueno et al. 2003).

3.2. Mechanical properties

The mechanical properties such as hardness (Vickers hardness and nano hardness) were analyzed in samples subjected to compression cycles to study the stress induced ε-martensite (Nascimento, 2008). Figure 10 shows the influence of austenite grain size in Vickers hardness and the nano hardness of the Fe-Mn-Si-Cr-Ni-Co alloy.

The Vickers hardness (Fig-10a) shows the contribution of ε-martensite and austenite phases simultaneously. In this case, the behavior is similar to that of the commercial austenitic steel, the Vickers hardness decreases as a function of grain size (Nascimento, 2008). Literature data indicated a linear relationship between the yield stress (σ) and the inverse of the square

root of grain diameter, according to Hall-Petch (Leslie, 1996), (Gladman, 1997). Using pyramidal indenter geometry it is possible to estimate the hardness (GPa) of these phases separately, Fig. 10(b) and Fig. 10(c).

The curve of hardness, Fig. 10(c) shows similar behavior to that of the austenite phase curve Fig. 10(a). But the martensitic phase, Fig. 10(b), shows an increased hardness due to increase in grain size. This result is explained by the fact that increased grain size makes shape

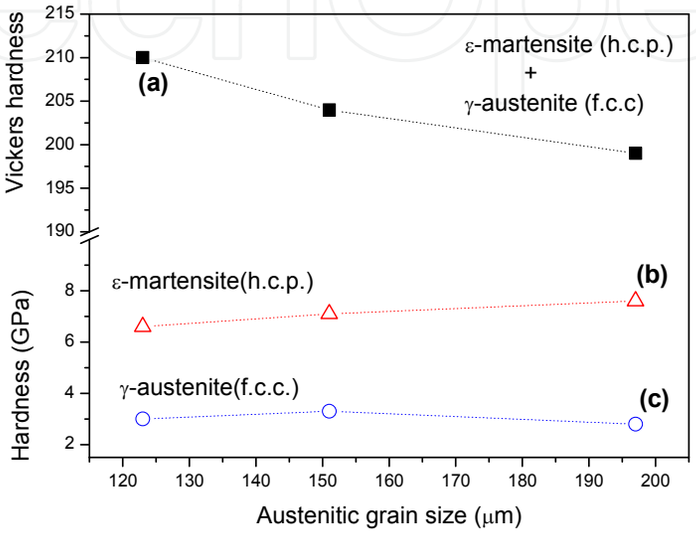

a)

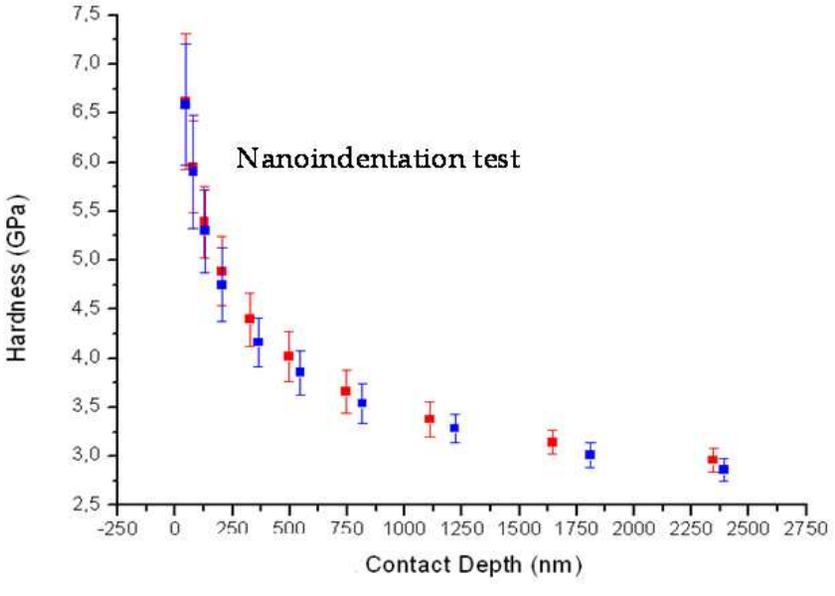

b)

Figure 10. a) Hardness (GPa) and Vickers hardness as a function of austenite grain size, recovery state, b) Hardness (GPa) curve obtained in nanoindentation tests in Fe-Mn-Si-Cr-Ni iron based shape memory alloy.

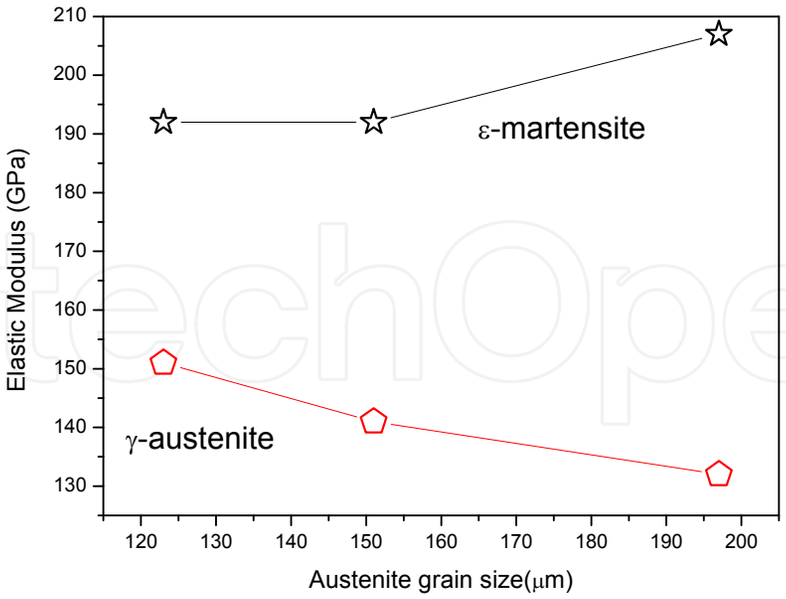

Figure 11. Effect of austenite grain size on the elastic modulus (GPa) to ε-martensite and austenite phases.

recovery more difficult. In this case, these samples have a higher volumetric fraction of ε-martensite residual, a phase which was not recovered at each cycle of thermomechanical treatment (Nascimento et al. 2003). Figure 10d shows the typical curve obtained in the nanoindentation test. The blue curve is the first training cycle and the red curve is the sixth cycle, or thermomechanical cycle. For small contact depths, hardness is analyzed on the surface of the material and for greater contact depths, the values of hardness are obtained in bulk, approaching conventional austenitic stainless steel.

The variations of the modulus of elasticity for the martensite and austenite phases are shown in Figure 11. For a commercial stainless steel the modulus of elasticity is around 210 GPa. When we analyze the phases separately, we observed a change in value. This variation is due to the difference in chemical composition and also alterations in the volumetric fraction of the phases.

4. Conclusion

The main conclusion of this study refers to the fact that the initial refinement of the microstructure in iron based alloys affects the performance of shape recovery of these materials. These changes occur in several aspects: morphology and microstructure of the phases, structural parameters, mechanical properties and shape memory effect. Changes in the ratio c/a of martensitic phase affect the reverse motion of partial dislocation that is also affected by grain size. Samples with larger grain size need to relax the strain by creating new guidelines facilitating the precipitation of the α'-martensite. Analysis using the Rietveld refinement are important because they allow better evaluation of the structural variations.

Author details

Fabiana Cristina Nascimento Borges
Universidade Estadual de Ponta Grossa, Departamento de Física – UEPG, Ponta Grossa, Paraná, Brazil

Acknowledgement

We would like to thank the Brazilian agency CNPq, Fapesp, AEB and Vilares Metals S.A. for its financial support, and the Phd. Jorge Otubo (ITA-SP-Brazil) and Phd. Paulo R. Mei (UNICAMP-SP-Brazil).

5. References

Araújo, L. A. ((Ed. Arte e Ciência). (1997)). *Manual de Siderurgia – Transformação*, Siemens.

Bergeon N, Guenin G, Esnouf C. (1997). Characterization of the stress-induced ε-martensite in a Fe-Mn-Si-Cr-Ni shape memory alloy: microstructural observation at different scales, mechanism of formation and growth. *Materials Science and Engineering A*. 1997; 238: 309-316.

Bueno J. C., Nascimento F. C., Otubo J., Lepienski C. M., Mei P. R. Development of phase identification by optical metallography with nanoindentation in shape memory alloys. In: *International Conference on Advanced in Materials and Processing Technologies*, 2006, Las Vegas. International Conference on Advanced in Materials and Processing Technologies, 2006. p. 01-04.

Bueno J. C., Nascimento F. C., Otubo J. (2003). Effect of training and the reduction of the austenitic grain size on the morphology of the stress-induced ε martensite in stainless SMAs. Cobem, 2003.

Gauzzi F, Montanari R. (1999). Martensite reversion in an Fe–21%Mn–0.1%Calloy. *Materials Science and Engineering A*. 273-275: 524-527.

Gladman, T. (1997). Microstructure property relationships. The physical metallurgy of microalloys steels, pp. 40.

Leslie, W.C. (1996). Physical metallurgy os steels. Physical Metallurgy, Chapter 17, Vol. II, pp. 1591.

Nascimento, F. C. (2008). *Ligas austeniticas com memória de forma- influência da microestrutura nas propriedades mecânicas e na recuperação de forma,* Edgar Blucher, ISBN 978-85-61209-38-4 São Paulo, Brazil.

Nascimento F. C., Mei P. R., Cardoso L. P., Otubo J. (2008). Grain size effect on the structural parameters of the stress induced epsilon hcp: martensite in iron-based shape memory alloy. *Materials Research*, Vol. 11, pp. 1516-1539, ISSN 1516-1439.

Nascimento F. C., Mei P. R., Otubo, J. (2003). Effects of grain size on the shape recovering properties of a stainless SMA. In: *Proceedings of Conference Advances in Materials and Processing technologies*, Las Vegas. 2003; 1436-1440.

Nascimento, F. C., Sorrila, F. V., Otubo, J., Mei P. R. (2003). Stainless shape memory alloys Microstructure by optical microsocpy using different etchants. Acta Microscopica, pp. 01-05.

Otubo J., Nascimento F. C., Mei P. R., Cardoso L. P., Kaufman M. (2002). Influence of austenite grain size on mechanical properties of stainless shape memory alloy. *Materials Transactions*, Vol. 43, pp. 916-919.

Vlack V., Vlack, Hall L. (1998). Princípios de Ciência dos Materiais. Edgar Blucher. pp.1-378.

IntechOpen